



Investigation on Optical Properties of Atmospheric Pressure Plasma Jets of N₂ Gas

Erkan İLİK^{1,*}, Çağrı DURMUŞ², Tamer AKAN³

¹*Eskisehir Osmangazi University, Faculty of Science and Letters, Department of Physics, TR-26040, Eskisehir, Turkey*

eilik@ogu.edu.tr, ORCID: 0000-0003-2986-0015

²*Eskisehir Osmangazi University, Graduate School of Sciences, TR-26040, Eskisehir, Turkey*

501320191006@ogrenci.ogu.edu.tr, ORCID: 0000-0003-0174-0580

³*Eskisehir Osmangazi University, Faculty of Science and Letters, Department of Physics, TR-26040, Eskisehir, Turkey*

akan@ogu.edu.tr, ORCID: 0000-0003-0907-2724

Received: 10.03.2020

Accepted: 07.05.2020

Published: 25.06.2020

Abstract

In this study, firstly, N₂ atmospheric pressure plasma jet (APPJ) system was presented. Nitrogen gas discharges are produced as jet using an AC power supply which can be adjusted between 6-18 kV and the frequency value of 13-20 kHz at atmospheric pressure. The change of length of produced atmospheric pressure nitrogen plasma jet, according to gas flow rate has been investigated and the produced jet length was approximately 2 cm for 5 L/min when the applied voltage was 18 kV and the frequency was 15 kHz. Nitrogen plasma jet produced at atmospheric pressure was examined with optical emission spectroscopy (OES) and the correlation between gas flow rate and emission spectra were investigated. Furthermore, electron temperature and electron density of atmospheric pressure nitrogen gas plasma jet were estimated under different flow rates of N₂ gas.

Keywords: Nitrogen; Atmospheric pressure plasma; N₂ APPJ; Electron temperature; Electron density.



N₂ Gazı Atmosferik Basınç Plazma Jetlerinin Optik Özelliklerinin İncelenmesi

Öz

Bu çalışmada öncelikle atmosferik basınçta plazma jet (APPJ) üretimine olanak sağlayan sistem tanıtılmıştır. Azot gazı deşarjları atmosferik basınçta 6-18 kV ve 13-20 kHz ayarlı AC güç kaynağı ile jet olarak üretilmiştir. Üretilen atmosferik basınç azot plazma jetin gaz akış hızına göre uzunluğunun değişimi incelenmiş olup, üretilen jet uzunluğu 5 L/dk gaz akış hızı, 18 kV voltaj ve 15 kHz frekans değerinde yaklaşık olarak 2 cm'dir. Atmosferik basınçta üretilen azot plazma jet, optik emisyon spektroskopisi (OES) ile incelenmiş ve gaz akış hızı ile emisyon spektrumlarındaki değişimler belirlenmiştir. Bununla birlikte, atmosferik basınç azot gazı plazma jetin elektron sıcaklığı ve elektron yoğunluğu azot gazının farklı gaz akış hızları için hesaplanmıştır.

Anahtar Kelimeler: Azot; Atmosferik basınç plazma; N₂ APPJ; Elektron sıcaklığı; Elektron yoğunluğu.

1. Introduction

Many studies have been carried out so far with gas discharge plasmas known as cold plasmas. Cold plasmas have many advantages such as the effects of low temperature, low electric field, and the chemical interactions of the active radicals have various applications. Cold plasmas are widely used in many applications such as sterilization, surface applications such as coating, activation, cleaning, polymerization, oxidation, nitriding, and medical treatments [1-4]. Instead of noble gases such as argon (Ar), helium (He), etc., nitrogen (N₂) gas has also used in these applications [5, 6]. Nitrogen gas plasmas have a vital importance because of the content of radical (reactive) and metastable particles. Molecular nitrogen does not react easily under normal conditions and is ineffective. However, the excited or dissociated N₂ species, especially atomic nitrogen (N) in the mixed gases containing N₂ or N₂⁺ caused many reactions to be used in important applications. Different excited states of species such as N₂, N₂⁺ and N are also formed in nitrogen plasmas and form important reactions [7]. The first excited state of nitrogen, the metastable triplet N₂(A³Σ_u⁺), has a threshold energy of 6.2 eV and a lifetime of about 2 seconds. From this point of view, it is an important energy carrier, so it plays an effective role in N₂ plasma by making important mechanisms such as ionization, decomposition, plasma chemistry and gas heating [8]. Although N₂(A) plays an important role in the basic processes controlling nitrogen discharge, it is known that the main energy storage is not by electronic metastable. It has been observed in previous studies that the N₂(X¹Σ_g⁺) state of the control mechanism is at vibration levels [9]. However, N atoms formed by the decomposition of nitrogen molecules used in metallic

nitriding are easily produced in nitrogen plasma. Observation of $N_2^+(B^2\Sigma_u^+ \rightarrow X^2\Sigma_g^+)$ transitions also indicates that N_2^+ is abundant [10]. Characteristic emissions and numerical calculations of species such as N_2 , N_2^+ , N^+ , and N in low- and atmospheric pressure of nitrogen luminescent (glow) discharges have been examined [11, 12]. N_2 and N_2^+ species in nitrogen plasma play vital role in synthesis of new functional and mechanical materials as they have strong chemical activity. Production of anti-microbial low density polyethylene films and hydrophilic polymer structures [13], processing of hydroxyl cellulose films [14], GaN nanostructures containing nano-wire and nano-particles [15], nitrogen oxide processing [16], production of high activity plasma welding for the storage of silicon nitride films [17], modification of amorphous SiO_2 nanoparticles [18], single crystal production [19], modification of stainless steel surfaces (ion implantation) [20], treatment of indium tin oxide (ITO) films [21], graphene and graphite structures [22], surface modification of polyacrylonitrile copolymer structures [23], diamond building carbon (DLC) production [24], annealing Ta_2O_5 films [25] are examples of applications of material processing of cold plasma produced with low pressure nitrogen gas/gas mixtures.

According to the literature, there are a lot of applications by using N_2 APPJs, but the basic characteristics of the produced plasma are not examined in detail. In order to do that, a jet system which produces nitrogen gas plasmas at atmospheric pressure is designed and produced. Firstly, the behavior of nitrogen gas plasma in atmosphere medium according to different gas flow rate was investigated. Then, optical emission spectra (OES) of nitrogen plasmas (N_2 APPJs) were taken depending on gas flow rate. The possible atomic and molecular transitions in nitrogen plasma were obtained from the OES data in accordance with the literature. Finally, electron temperature (T_e) and electron density (n_e), which are one of the main parameters of nitrogen gas plasma, were calculated by Boltzmann two-line method. It is considered that this study would be a basis for determining the appropriate gas flow rate for N_2 plasmas in further experimental studies.

2. Materials and Methods

Designed system to produce N_2 APPJs and the scheme of N_2 APPJ system were given in Fig. 1 and Fig. 2, respectively. The atmospheric pressure plasma system used here is known as plasma jet.

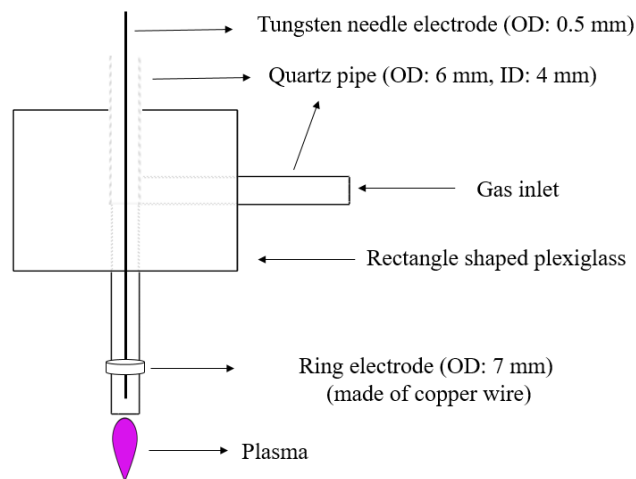


Figure 1: A schematic of N₂ atmospheric pressure plasma jet device

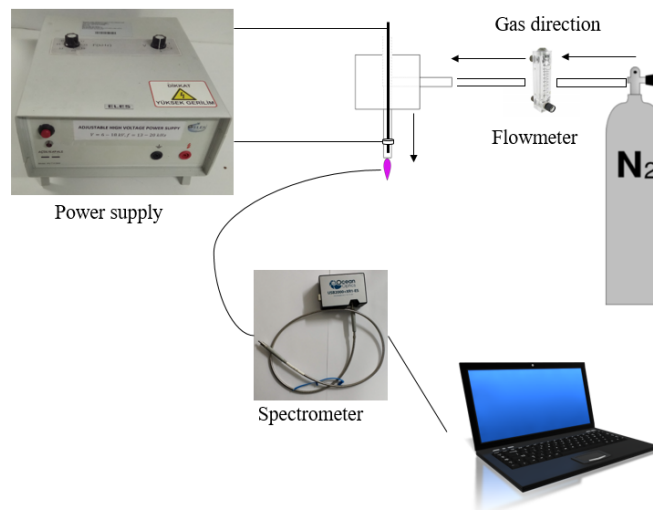


Figure 2: Close up view of APPJ system

The whole system was installed in a fume hood to protect against the stifling effects of nitrogen gas. In order to generate APPJ, three identical quartz glass pipes (OD: 6 mm, ID: 4 mm) were used. First pipe which was used as gas inlet was fixed on rectangle shaped plexiglass (50x25x37 mm). Other pipe which was fixed on the plexiglass was used to hold tungsten electrode. The tungsten electrode was extended approximately 3 mm to the nozzle of the pipe attached to gas outlet. The tungsten wire has 0.5 mm thickness. The distance of the ring electrode to the nozzle of the pipe was determined as a result of making a series of attempts. A ring electrode which was made of copper was connected to the end of the glass pipe. Then, a gas flowmeter (LZT M-6 flowmeter, 2-10 L/min) was connected to control gas flow rate to gas inlet of the system. Gas outlet of the pipe was mounted with pneumatic hose (OD: 10 mm, ID: 6 mm).

Nitrogen gas cylinder (Habas 99.999% purity) and its regulator were used to supply gas to the APPJ system. The connection between this gas cylinder and the fume hood is provided by a 6.5 mm diameter pneumatic hose. The alternating current (AC) power supply (ELES HV-711GK4), which can be adjusted between 6-18 kV and the frequency value of 13-20 kHz, was used for generating N₂ APPJ.

A spectrometer (Ocean Optics USB2000+), fiber optic cable and computer program (OceanView software) were used in order to examine the spectroscopic properties of N₂ APPJ as can be seen in Fig. 1. 10 mm wide slit (300 grooves/mm grating, the spectral resolution = 0.1 nm) were used to measure spectra in the sensitive range from 200-1100 nm. In order to avoid fluctuation of intensity, integration time of OES was fixed at 1 s through the experiment, and optical emission spectrometer was recalibrated priorly each measurement.

3. Results

In order to generate N₂ APPJ, the high voltage input was connected to the tungsten needle electrode. A ring electrode which was made of copper was connected to the end of the glass pipe. Then, N₂ gas was flowed through the glass pipe in the middle of the plexiglass. Gas sent from the nitrogen gas cylinder was read out from gas flowmeter, simultaneously. After all, when the AC voltage was applied between the electrodes, the nitrogen discharge was generated between the electrodes. When the flow rate of nitrogen gas was set at a certain value, the nitrogen gas discharge between the electrodes emerges as a N₂ APPJ. At different gas flow rates, generated N₂ APPJ was shown in Fig. 3.

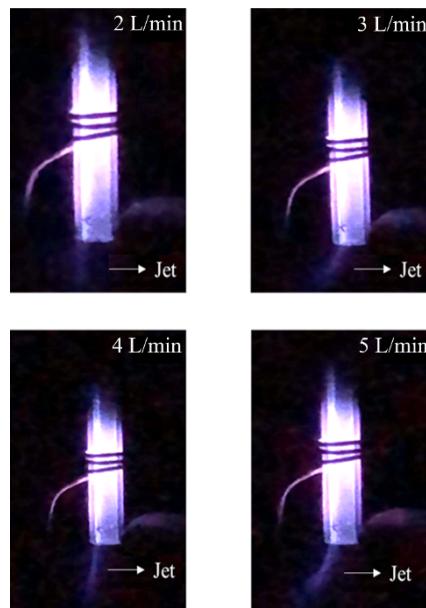


Figure 3: Atmospheric pressure nitrogen gas plasma jet photographs for different N₂ flow rates

We have achieved the longest jet length (about 2 cm) at 18 kV-15 kHz in N₂ APPJs that we produced in a similar diameter before. When we reduce the voltage to less than 18 kV, there is a decreasing in the intensity of the jet, thus its length. On the other hand, if we increase the frequency above 15 kHz, it turned to more intense plasma but similarly jet length decreased. Moreover, when the frequency value was adjusted below 15 kHz, the jet becomes unstable and discontinuous form. The distance between the ring electrode and the nozzle was set at 3 cm. Proper adjustment of this distance prior to the experiment affects the structure of the plasma formed in the atmosphere. It was seen that when the distance between the electrodes decreased, the plasma transformed into an arc form with a high intensity, in other respects when it increased, plasma formed only between the electrodes and could not reach the atmosphere.

The change of plasma jet length that can be released into the atmosphere according to the gas flow rate was also shown in the Fig. 4.

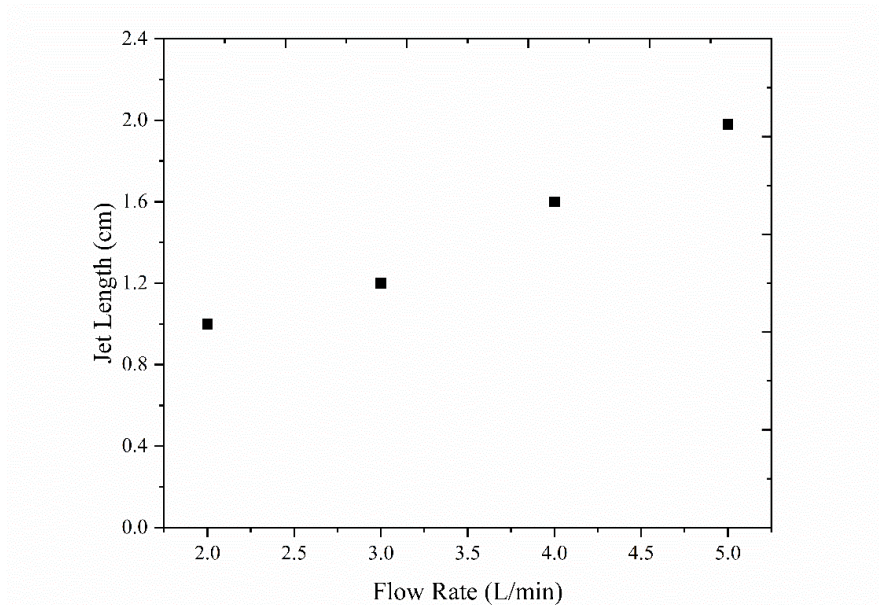


Figure 4: The change of plasma jet length according to the gas flow rate

As shown in Fig. 3 and Fig. 4, the length of APPJ was proportional to gas flow rate. This situation was related with high pressure formed inside the glass pipe. It was observed that high pressure nitrogen gas mixed with the atmosphere medium had been seen to ionize more easily. Spectra taken from the same distance of the N₂ APPJs were shown in Fig. 5.

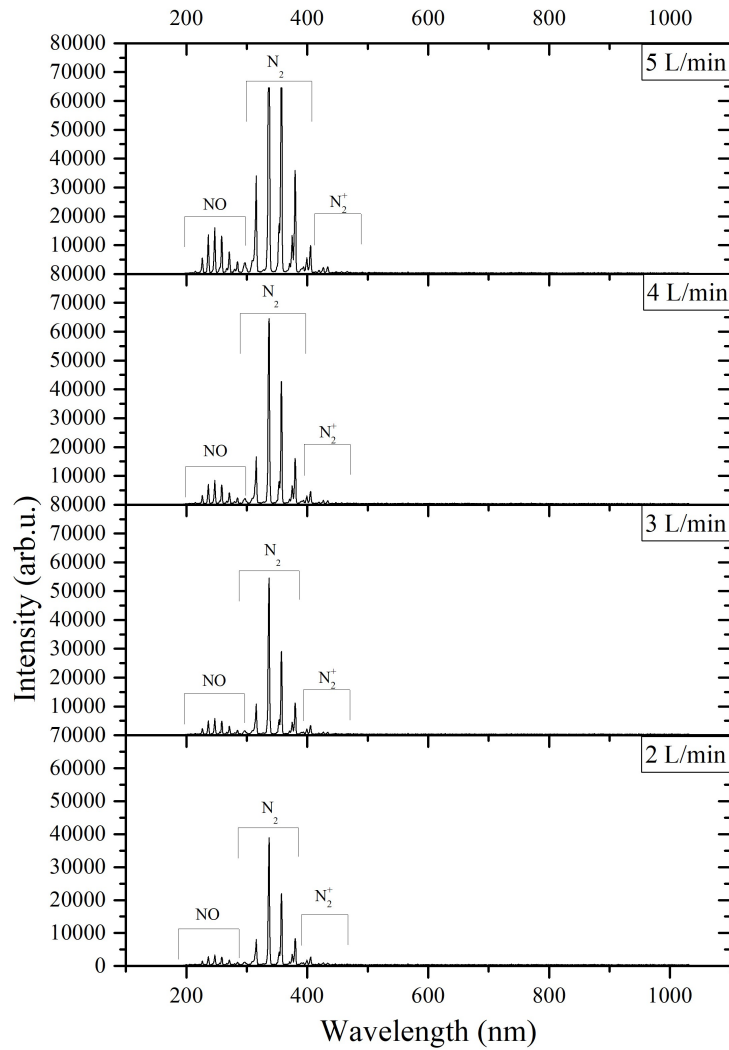


Figure 5: The optical emission spectra of N₂ APPJ at different gas flow rates

In the optical emission spectra taken for different nitrogen gas flow rates, various atom/atoms, molecules and radical particles were found in the N₂ APPJs [26]. Here, it was observed that the NO radical concentration was proportional to gas flow rate. Stated in other words, the NO radical concentration increases as gas flow rate increases. OH radicals (at 308 nm) were dominated by the NO radicals. Therefore, the wavelength corresponding to the OH radicals in the optical emission spectra was not marked and was only given in Table 1. The intensity of N atoms (747 - 870 nm) was determined to be quite low compared to other species such as N₂, N₂⁺, etc. On the other hand, N₂ and N₂⁺ peaks were observed to increase continuously up to 5 L/min (Fig. 6). As a result of ionization of nitrogen gas, this is an expected result and it is clearly seen from the Fig. 6 that ionization increases with increasing gas flow rate.

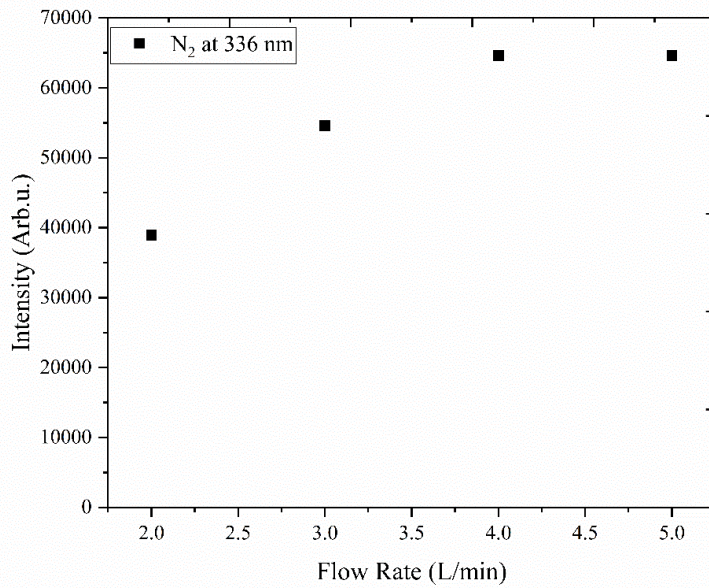


Figure 6: Change of N₂ emissions depending on gas flow rate

Furthermore, OES device used during the measurement reached the upper count limit at a flow rate of 5 L/min. When working in atmosphere medium, wavelengths of H, N and O are expected to be seen in the spectra. However, since the OH and NO radicals were formed by the interaction of H, N, and O atoms, these atoms were not directly observed in the spectra. OH and NO intensities were supposed to be suppressed by N₂. Observed transitions in N₂ APPJs were given in Table 1.

Table 1: Observed atomic and molecular transitions in N₂ APPJ [26]

| Plasma Component | Wavelength (nm) | Transition | Excitation Energy (eV) |
|-----------------------------|-----------------|---------------------------------------------------------------------------------------------------------|------------------------|
| NO | 204.70 | A ² Σ ⁺ , (v=2) – X, (v=0) | ~5.46 |
| | 214.80 | A ² Σ ⁺ , (v=1) – X, (v=0) | ~5.46 |
| | 226.20 | A ² Σ ⁺ , (v=0) – X, (v=0) | ~5.46 |
| NO | 236.30 | A ² Σ ⁺ , (v=0) – X, (v=1) | ~5.46 |
| | 247.10 | A ² Σ ⁺ , (v=0,) – X, (v=2) | ~5.46 |
| | 258.70 | A ² Σ ⁺ , (v=0) – X, (v=3) | ~5.46 |
| | 271.30 | A ² Σ ⁺ , (v=0) – X, (v=4) | ~5.46 |
| OH | 308.00 | A ² Σ ⁺ (v=0), – X ² Π, (v=0) | 9,10 |
| | 315.90 | C ³ Π _u , (v=1) – B ³ Π _g , (v=0) | 11.30 |
| | 337.10 | C ³ Π _u , (v=0) – B ³ Π _g , (v=0) | 11.00 |
| | 353.60 | C ³ Π _u , (v=1) – B ³ Π _g , (v=2) | 11.30 |
| | 357.70 | C ³ Π _u , (v=0) – B ³ Π _g , (v=1) | 11.00 |
| N ₂ | 370.90 | C ³ Π _u , (v=2) – B ³ Π _g , (v=4) | 11.50 |
| | 375.40 | C ³ Π _u , (v=1) – B ³ Π _g , (v=3) | 11.30 |
| | 380.40 | C ³ Π _u , (v=0) – B ³ Π _g , (v=2) | 11.00 |
| | 399.70 | C ³ Π _u , (v=1) – B ³ Π _g , (v=4) | 11.30 |
| | 405.80 | C ³ Π _u , (v=0) – B ³ Π _g , (v=3) | 11.00 |
| | 434.30 | C ³ Π _u , (v=0) – B ³ Π _g , (v=4) | 11.00 |
| | 391.40 | B ² Σ _u ⁺ , (v=0) – X ² Σ _g ⁺ , (v=0) | 18.70 |
| N ₂ ⁺ | 427.80 | B ² Σ _u ⁺ , (v=0) – X ² Σ _g ⁺ , (v=1) | 18.70 |
| | 470.90 | B ² Σ _u ⁺ , (v=0) – X ² Σ _g ⁺ , (v=2) | 18.70 |
| | 746.80 | 3s ⁴ P – 3p ⁴ S ⁰ | 11.90 |
| N | 870.30 | 3s ⁴ P – 3p ⁴ D ⁰ | 11.80 |

In the non-LTE plasmas, the electron temperature (T_e) can be calculated using Boltzmann approximation [27].

$$T_e = \frac{E_2 - E_1}{k} \left[\ln \left(\frac{A_2 g_2 I_1 \lambda_1}{A_1 g_1 I_2 \lambda_2} \right) \right]^{-1} \quad (1)$$

Here, sub index 1 and 2 correspond to two different electronic states of N_2 . E_1 and E_2 represent the energy levels. λ_1 and λ_2 are wavelengths of emitted photons; I_1 and I_2 are measured relative intensities. g_1 and g_2 represent the statistical weights of these levels. A_1 and A_2 represent the transition probabilities. Furthermore, the electron density can be estimated as follows [28]:

$$n_e \cong 10^{18} T Z^{7/2} \left(\frac{1}{n_a} \right)^2 \left(\frac{2}{n_b} \right)^5 \text{ cm}^{-3} \quad (2)$$

In Eqn. (2), n_b and n_a are the level of excited state and ground state, respectively. T is the electron temperature. Electron temperature of N_2 APPJ was estimated with using N atoms (at 747 nm and 870 nm) and the values of T_e varied from 0.19 eV to 0.31 eV for different gas flow rates as can be seen in Fig. 7. The electron densities for different gas flow rates were also calculated as can be seen in Fig. 8. The measurement results obtained in the experiment for this calculation are given in Table 2.

Table 2: Data used in electron temperature calculation

| Flow Rate | Wavelength (nm) | Intensity (Arb.u.) | $A_1 g_1$ (s^{-1}) | $A_2 g_2$ (s^{-1}) | E_1 (eV) | E_2 (eV) |
|-----------|-----------------|--------------------|------------------------|------------------------|------------|------------|
| 2 L/min | 746 | 379 | 7.84×10^7 | - | 11.9 | - |
| | 870 | 362 | - | 4.32×10^7 | - | 11.75 |
| 3 L/min | 746 | 377 | 7.84×10^7 | - | 11.9 | - |
| | 870 | 300 | - | 4.32×10^7 | - | 11.75 |
| 4 L/min | 746 | 376 | 7.84×10^7 | - | 11.9 | - |
| | 870 | 393 | - | 4.32×10^7 | - | 11.75 |
| 5 L/min | 746 | 434 | 7.84×10^7 | - | 11.9 | - |
| | 870 | 332 | - | 4.32×10^7 | - | 11.75 |

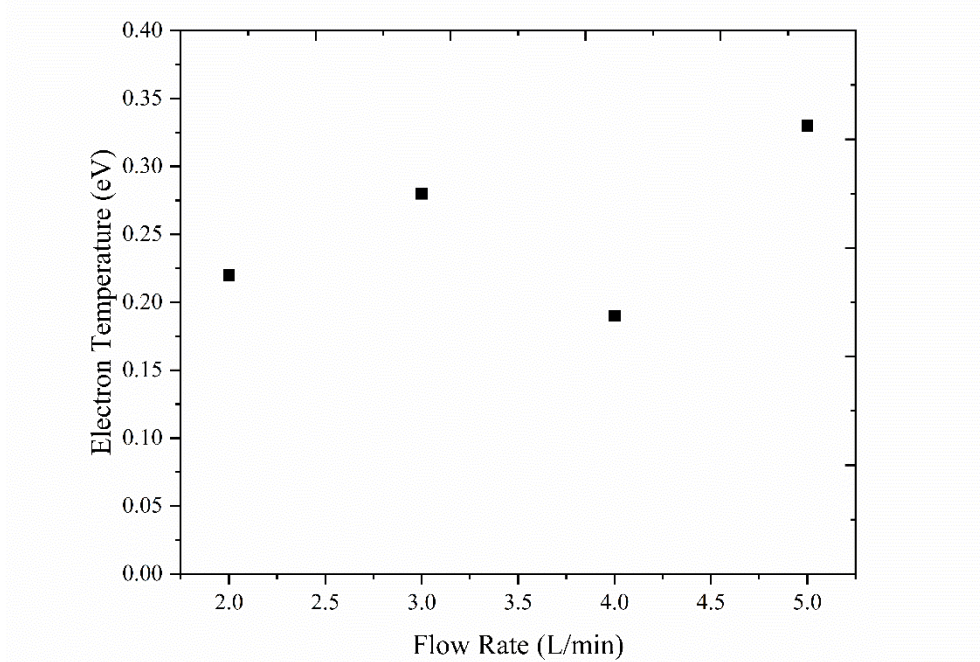


Figure 7: Electron temperature changing according to gas flow rate

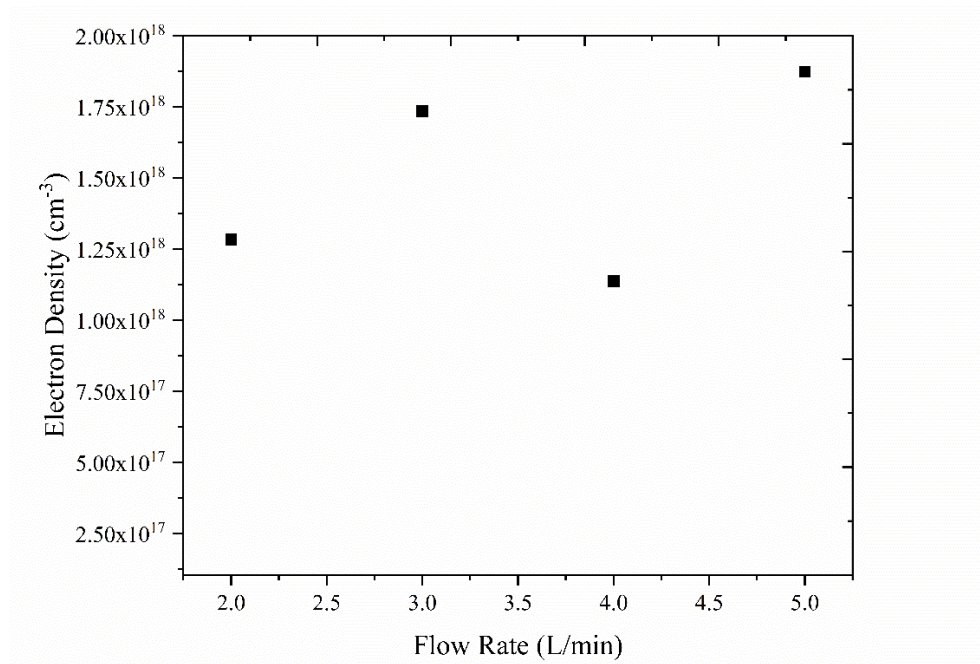


Figure 8: Electron density according to gas flow rate

As N₂ gas flow rate increased, there was no linear change in electron temperature. It is assumed that this result is due to the production of N₂ APPJ in the fume hood. At high gas flow rates, the jet draws towards the top of the furnace and leans towards the nearest electrode. Here, the outgoing plasma jet may tend to make a new ionization line. Since this ionization line can generate new types of reactions, it is thought that such variations are occurred in temperature

calculations. Similar to the change of electron temperature, as N₂ gas flow rate increased, there was no linear change in electron temperature. The electron densities obtained from the N₂ APPJ were between $1.14 \times 10^{18} \text{ cm}^{-3}$ and $1.87 \times 10^{18} \text{ cm}^{-3}$ values. It is thought that the reason for the decrease of electron density at high gas flow rates (especially at 4 L/min) is due to the ionization of gas atoms by free electrons. Similar results were obtained as the experiments were repeated. Calculated T_e and n_e values in accordance with the literature [27].

4. Conclusions

In this study, atmospheric pressure nitrogen gas plasmas (N₂ APPJs) were produced as a jet. The experiments were carried out in fume hood in order to protect from the effects of harmful gases which may occur in N₂ APPJs produced in atmospheric medium. The production of nitrogen gas plasma jet is quite difficult in comparison to noble gases. However, we have successfully produced plasma jet longer than 2 cm by using the alternating current power supply. The length of the jet was closely related to gas flow rate. It was determined that the jet length increased in proportion to the increase in gas flow rate. At high gas flow rates, APPJ bended towards the nearest electrode. The longest jet was observed at a gas flow rate of 4-5 L/min. However, therefore bending has also occurred at these flow rates. As the connection part of the ring electrode to the power supply in the system was close to the nozzle, it has been observed that the ionization line was directed towards this electrode as the length of the jet increases. The distance of the ring electrode to the end of the pipe was determined by trial and error. Plasma arc formation was observed if the ring electrode was close to the nozzle of the tube, and jet formation was not observed if the ring electrode was away from the nozzle of the tube. After that, the optical emission spectra were taken from 0.5 cm distance of the N₂ APPJ system. In the obtained spectra, as gas flow rate increased, N₂, N₂⁺, and NO peaks increased proportionally. In addition, the OH peaks increased depending on gas flow rate, but these peaks were dominated by NO. Therefore, the wavelength corresponding to the OH radicals in the optical emission spectra was not marked and was only given in Table 1. Furthermore, electron temperature and electron density were calculated according to gas flow rate by using spectral line intensities of N atoms. Although the nitrogen gas flow rate increased, there was a relatively small increase in electron temperature, but a linear increase was not achieved. At the same time, the outgoing jet was trying to make a new ionization line. This is thought to increase the electron temperature and hence the electron density. Detailed studies on the electrical properties of N₂ plasma jet applications, in particular voltage and frequency changes, are planned for the future.

Acknowledgement

This study is supported by Eskisehir Osmangazi University Scientific Research Committee with project number 201819012.

References

- [1] Bogaerts, A., Neyts, E., Gijbels, R., Van der Mullen, J., *Gas discharge plasmas and their applications*, Spectrochimica Acta Part B: Atomic Spectroscopy, 57(4), 609-658, 2002.
- [2] Petitpas, G., Rollier, J.-D., Darmon, A., Gonzalez-Aguilar, J., Metkemeijer, R., Fulcheri, L., *A comparative study of non-thermal plasma assisted reforming technologies*, International Journal of Hydrogen Energy, 32(14), 2848-2867, 2007.
- [3] Tendero, C., Tixier, C., Tristant, P., Desmaison, J., Leprince, P., *Atmospheric pressure plasmas: a review*, Spectrochimica Acta Part B: Atomic Spectroscopy, 61(1), 2-30, 2006.
- [4] Treumann, R.A., Klos, Z., Parrot, M., *Physics of electric discharges in atmospheric gases: an informal introduction*, Planetary Atmospheric Electricity, Springer New York, 133-148, 2008.
- [5] Ahmed, K., Allam, T., El-sayed, H., Soliman, H., Ward, S., Saied, E., *Design, construction and characterization of ac atmospheric pressure air non-thermal plasma jet*, Journal of Fusion Energy, 33(6), 627-633, 2014.
- [6] Allam, T., Ward, S., El-Sayed, H., Saied, E., Soliman, H., Ahmed, K., *Electrical parameters investigation and zero flow rate effect of nitrogen atmospheric nonthermal plasma jet*, Energy and Power Engineering, 6(12), 437, 2014.
- [7] Ricard, A., Oh, S.G., Jang, J., Kim, Y.K., *Quantitative evaluation of the densities of active species of N₂ in the afterglow of Ar-embedded N₂ RF plasma*, Current Applied Physics, 15(11), 1453-1462, 2015.
- [8] Ricard, A., Oh, S.-g., Guerra, V., *Line-ratio determination of atomic oxygen and N₂(A₃Σ_u⁺) metastable absolute densities in an RF nitrogen late afterglow*, Plasma Sources Science Technology, 22(3), 2013.
- [9] Guerra, V., Sa, P., Loureiro, J., *Role played by the N₂(A₃Σ_u⁺) metastable in stationary N₂ and N₂-O₂ discharges*, Journal of Physics D: Applied Physics, 34(12), 1745, 2001.
- [10] Loureiro, J., Sá, P., Guerra, V., *Role of long-lived N₂(X¹Σ_g⁺, v) molecules and N₂(A₃Σ_u⁺) and N₂(a¹Σ_u⁻) states in the light emissions of an N₂ afterglow*, Journal of Physics D: Applied Physics, 34(12), 1769, 2001.
- [11] Hrycak, B., Jasiński, M., Mizeraczyk, J., *Spectroscopic characterization of nitrogen plasma generated by waveguide-supplied coaxial-line-based nozzleless microwave source*, IOP Publishing, 406(1), 012037, 2012.
- [12] Rankovic, D., Kuzmanovic, M., Pavlovic, M.S., Stoiljkovic, M., Savovic, J., *Properties of argon–nitrogen atmospheric pressure DC arc plasma*, Plasma Chemistry and Plasma Processing, 35(6), 1071-1095, 2015.
- [13] Karam, L., Casetta, M., Chihib, N.E., Bentiss, F., Maschke, U., Jama, C., *Optimization of cold nitrogen plasma surface modification process for setting up antimicrobial low density polyethylene films*, Journal of the Taiwan Institute of Chemical Engineers, 64, 299-305, 2016.
- [14] Mahmoud, K., *Optical properties of hydroxyethyl cellulose film treated with nitrogen plasma*, Spectrochimica Acta Part A: Molecular and Biomolecular Spectroscopy, 157, 153-157, 2016.

- [15] Gholampour, M., Abdollah-Zadeh, A., Shekari, L., Poursalehi, R., *From nanoparticles to nanowires of GaN with different hydrogen gas flow rates by PDC-PECVD*, *Procedia Materials Science*, 11, 304-308, 2015.
- [16] Choi, J.S., Park, J.G., *Interface characterization of nitrogen plasma-treated gate oxide film formed by RTP technology*, *Surface and Interface Analysis*, 46(S1), 303-306, 2014.
- [17] Shi, D., Xu, W., Miao, C., Ma, C., Ren, C., Lu, W., Zhang, Q., *A high-activity nitrogen plasma flow source for deposition of silicon nitride films*, *Surface and Coatings Technology*, 294, 194-200, 2016.
- [18] Pan, G.-T., Chong, S., Yang, T.C.-K., Yang, Y.-L., Arjun, N., *Surface modification of amorphous SiO₂ nanoparticles by oxygen-plasma and nitrogen-plasma treatments*, *Chemical Engineering Communications*, 203(12), 1666-1670, 2016.
- [19] Wang, J.C., Ye, Y.R., Lin, Y.H., *Light-addressable potentiometric sensor with nitrogen-incorporated ceramic Sm₂O₃ membrane for chloride ions detection*, *Journal of the American Ceramic Society*, 98(2), 443-447, 2015.
- [20] Castro-Colin, M., Durrer, W., López, J.A., Ramirez-Homs, E., *Surface modification by nitrogen plasma immersion ion implantation on austenitic AISI 304 stainless steel*, *Journal of Iron and Steel Research International*, 23(4), 380-384, 2016.
- [21] Praveen, T., Shiju, K., Predeep, P., *Influence of plasma treatment on Indium Tin Oxide electrodes*, *Microelectronic Engineering*, 131, 8-12, 2015.
- [22] Bertóti, I., Mohai, M., László, K., *Surface modification of graphene and graphite by nitrogen plasma: Determination of chemical state alterations and assignments by quantitative X-ray photoelectron spectroscopy*, *Carbon*, 84, 185-196, 2015.
- [23] Pal, D., Neogi, S., De, S., *Surface modification of polyacrylonitrile co-polymer membranes using pulsed direct current nitrogen plasma*, *Thin Solid Films*, 597, 171-182, 2015.
- [24] Khatir, S., Hirose, A., Xiao, C., *Characterization of physical and biomedical properties of nitrogenated diamond-like carbon films coated on polytetrafluoroethylene substrates*, *Diamond and Related Materials*, 58, 205-213, 2015.
- [25] Alers, G., Fleming, R., Wong, Y., Dennis, B., Pinczuk, A., Redinbo, G., Urdahl, R., Ong, E., Hasan, Z., *Nitrogen plasma annealing for low temperature Ta₂O₅ films*, *Applied physics letters*, 72(11), 1308-1310, 1998.
- [26] <https://www.nist.gov/pml/atomic-spectra-database>, 06.03.2020.
- [27] Shah, M., Ahmad, R., Iikhlaq, U., Saleem, S., *Characterization of pulsed DC nitrogen plasma using optical emission spectroscopy and Langmuir probe*, *Journal of Natural Sciences and Mathematics*, 53, 1-12, 2013.
- [28] Marr, G.V., *Plasma spectroscopy*, Elsevier Publishing Company, 5, 1968.